"Separated" versus "Contact" Ion-Pair Structures in Solution from Their Crystalline States: Dynamic Effects on Dinitrobenzenide as a Mixed-Valence Anion

ARTICLE *in* JOURNAL OF THE AMERICAN CHEMICAL SOCIETY · MARCH 2005

Impact Factor: 12.11 · DOI: 10.1021/ja043998x · Source: PubMed

5 AUTHORS, INCLUDING:

Sergiy V Rosokha
Roosevelt University
70 PUBLICATIONS **2,319** CITATIONS
SEE PROFILE

Ivan S. Neretin
48 PUBLICATIONS **821** CITATIONS
SEE PROFILE

J|A|C|S
ARTICLES
Published on Web 01/25/2005

"Separated" versus "Contact" Ion-Pair Structures in Solution from Their Crystalline States: Dynamic Effects on Dinitrobenzenide as a Mixed-Valence Anion

Jian-Ming Lü, Sergiy V. Rosokha, Sergey V. Lindeman, Ivan S. Neretin, and Jay K. Kochi*

Contribution from the Chemistry Department, University of Houston, Houston, Texas 77204-5003

Received October 1, 2004; E-mail: jkochi@uh.edu

Abstract: Qualitative structural concepts about dynamic ion pairs, historically deduced in solution as labile *solvent-separated* and *contact* species, are now quantified by the low-temperature isolation of crystalline (reactive) salts suitable for direct X-ray analysis. Thus, dinitrobenzenide anion (DNB^-) can be prepared in the two basic ion-paired forms by potassium-mirror reduction of *p*-dinitrobenzene in the presence of macrocyclic polyether ligands: L_C (cryptand) and L_E (crown-ethers). The crystalline "separated" ion-pair salt isolated as $K(L_C)^+//DNB^-$ is crystallographically differentiated from the "contact" ion-pair salt isolated as $K(L_E)^+DNB^-$ by their distinctive interionic separations. Spectral analysis reveals pronounced near-IR absorptions arising from intervalence transitions that characterize dinitrobenzenide to be a prototypical mixed-valence anion. Most importantly, the unique patterns of vibronic (fine-structure) progressions that also distinguish the "separated" from the "contact" ion pair in the crystalline solid state are the same as those dissolved into THF solvent and ensure that the same X-ray structures persist in solution. Moreover, these distinctive NIR patterns are assigned with the aid of Marcus−Hush (two-state) theory to the "separated" ion pair in which the unpaired electron is equally delocalized between both NO_2-centers in the symmetric ground state of dinitrobenzenide, and by contrast, the asymmetric electron distribution inherent to "contact" ion pairs favors only that single NO_2-center intimately paired to the counterion. The labilities of these dynamic ion pairs in solution are thoroughly elucidated by temperature-dependent ESR spectral changes that provide intimate details of facile isomerizations, ionic separations, and counterion-mediated exchanges.

Introduction

Intramolecular electron transfer has been extensively studied with different donor **D** and acceptor **A** dyads connected via molecular spacers, i.e., **D**(bridge)**A**[1] (also referred to as generic D(b)A systems[2]) owing to their relevance to biochemical assemblies, electron-transfer theory, molecular electronics, etc.[3−5] Of these, the mixed-valence systems with $\Delta G^\circ_{ET} = 0$ and comprised of single donor/acceptor entities provide the opportunity to examine systematically the structural effects of the redox centers as well as the bridge on electron-transfer rates in $\mathbf{D}(b)\mathbf{D}^{+\bullet}$ or $\mathbf{A}(b)\mathbf{A}^{-\bullet}$ systems.[6,7] Indeed, the discrete character of such organic mixed-valence systems is particularly useful in quantitatively elucidating the influence of (i) ion-pair structures and thermodynamics[8] as well as (ii) partial electron transfer (delocalization)[9] and reactivity of cationic ($\mathbf{D}/\mathbf{D}^{+\bullet}$) and anionic ($\mathbf{A}/\mathbf{A}^{-\bullet}$) redox centers.

One of the earliest and interesting examples of an organic mixed-valence system is dinitrobenzene anion radical (with a *p*-phenylene bridge connecting the $NO_2/NO_2^{-\bullet}$ redox dyads),

(1) Jortner, J., Bixon, M., Eds. *Electron Transfer − From Isolated Molecules to Biomolecules. Part 1, Adv. Chem. Phys.* **1999**, *10*, 6.
(2) (a) Newton, M. D. In *Electron Transfer in Chemistry*; Balzani, V., Ed.; Wiley-VCH: NY, 2001; Vol. 1, p 3. (b) Paddon-Row, M. N. *Acc. Chem. Res.* **1994**, *27*, 18.
(3) (a) Gray, H. B., Winkler, J. R., Eds. In *Biological and Artificial Supramolecular Systems*; Balzani, V., Ed.; Electron Transfer in Chemistry, Vol. III; Wiley-VCH: NY, 2001. (b) Wasielewski, M. R. *Chem. Rev.* **1992**, *92*, *435*. (c) Antolovich, M.; Keyte, P. J.; Oliver, A. M.; Paddon-Row: M. N.; Kroon, J.; Verhoeven, J. W.; Jonker S. A.; Warman J. M. *J. Phys. Chem.* **1991**, *95*, 1933. (d) Kilsa K.; Kajanus J.; Macpherson, A. N.; Martensson, J.; Albinsson, B. *J. Am. Chem. Soc.* **2001**, *123*, 3069. (e) Lewis, F. D.; Liu, J.; Weigel, W.; Rettig, W.; Kurnikov, I. V.; Beratan, D. N. *Proc. Natl. Acad. Sci. U.S.A.* **2002**, *99*, 12536.
(4) (a) Chen, P.; Duesing, R.; Graff, D. K.; Meyer T. J. *J. Phys. Chem.* **1991**, *95*, 5850. (b) Oevering, H.; Paddon-Row, M. N.; Hepperen, M.; Oliver, A. M.; Cotsaris, E.; Verhoeven, J. W.; Hush, N. S. *J. Am. Chem. Soc.* **1987**, *109*, 3258 (c) Liang, N.; Miller, J. R.; Closs, G. L. *J. Am. Chem. Soc.* **1989**, *111*, 8740. (d) Pullen, S. H.; Edington, M. D.; Studer-Martinez, S. L.; Simon, J. D.; Staab, H. A. *J. Phys. Chem. A* **1999**, *103*, 2740. (e) Penfield, K. W.; Miller, J. R.; Paddon-Row, M. N.; Cotsaris, E.; Oliver, A. M.; Hush, N. S. *J. Am. Chem. Soc.* **1987**, *109*, 5061. (f) Arimura, T.; Ide, S.; Suga, Y.; Nishioka, T.; Murata, S.; Tachiya, M.; Nagamura, T.; Inoue, H. *J. Am. Chem. Soc.* **2001**, *123*, 10744. (g) Newton, M. D. *Coord. Chem. Rev.* **2003**, *238−239*, 167. (h) Demadis, K. D.; Hartshorn, C. M.; Meyer, T. J. *Chem. Rev.* **2001**, *101*, 2655. (i) Daub, J.; Engl, R.; Kurzawa, J.; Miller, S. E.; Schneider, S.; Stockmann, A.; Wasielewski, M. R. *J. Phys. Chem. A* **2001**, *105*, 5655. (j) Davis, W. B.; Ratner, M. A.; Wasielewski, M. R. *J. Am. Chem. Soc.* **2001**, *123*, 7877.
(5) de Silva, A. P., Ed. In *Molecular Level Electronics*; Balzani, V., Ed.; Electron Transfer in Chemistry, Vol. 5, Part 1; Wiley-VCH: NY, 2001.
(6) (a) Liang, N.; Miller, J. R.; Closs, G. L. *J. Am. Chem. Soc.* **1990**, *112*, 5353. (b) Rak, S. F.; Miller, L. L. *J. Am. Chem. Soc.* **1992**, *114*, 1388. (c) Gautier, N.; Dumur, F.; Lloveras, J.; Vidal-Gancedo, J.; Veciana, C.; Rovira, P.; Hudhomme *Angew. Chem., Int. Ed.* **2003**, *42*, 2765. (d) Lahlil, K.; Moradpour, A.; Bowlas, C.; Menou, F.; Cassoux, P.; Bonvoisin, J.; Launay, J.-P.; Dive, G.; Dehareng, D. *J. Am. Chem. Soc.* **1995**, *117*, 9995. (e) Rosokha, S. V.; Sun, D.-L.; Kochi, J. K. *J. Phys. Chem. A* **2002**, *106*, 2283. (f) Sun, D.-L.; Rosokha, S. V.; Kochi, J. K. *J. Am. Chem. Soc.* **2004**, *126*, 1388.

and ESR studies over the past 50 years have led to the provocative conclusion that at least two distinctive anions exist in solution dependent on their mode of preparation with different countercations (M^+), solvent polarities, etc.[10] Species A with the unpaired electron equally delocalized between both nitro groups was assigned to the "free" anion ($DNB^{-\bullet}$) and/or a loosely bound, "separated" ion pair ($M^+//DNB^{-\bullet}$).[11] Conversely, the ESR spectrum of the second species (B) consisting of a major hyperfine splitting to only a single nitro-center was assigned to a tightly bound, "contact" ion pair ($M^+DNB^{-\bullet}$).[12] Recently, Nelsen and co-workers[13] showed that the diagnostic near-IR absorption band can be quantitatively analyzed by the two-state Marcus−Hush model as a delocalized system in which the unpaired electron resides in a single potential-energy well. Such a dinitrobenzenide anion would correspond to the free and/or separated ion pair consistent with the delocalized species A observed in the early ESR studies.[10,11] If so, the identity and nature of the contact ion pair (species B) remain open for questions.[14] Moreover, it is important to emphasize that the generalized concept of "solvent-separated" and "contact" ion pairs pertains to binary species extant in solution,[15] and the structures of such assemblies can only be qualitatively *inferred* from the solution (spectral) measurements. By contrast, X-ray crystallography of such highly reactive ion-pair salts can provide definitive structural information but requires the difficult isolation of single crystals and therefore have heretofore eluded a direct (unambiguous) tie-in to the ubiquitous solution data.

We showed in Part I[16] how the isolation of alkali-metal salts of the parent nitrobenzenide ($NB^{-\bullet}$) as both the crystalline separated ion pair and the corresponding contact ion pair[17] is made possible by the use of cyclic polyether ligands (L) during one-electron reduction of nitrobenzene with alkali-metal mirrors.[18] Thus, ion-pair separation is *enforced* via complete K^+ encapsulation with the three-dimensional [2,2,2] cryptand[19] so that the anion is effectively insulated from the complexed cation in solvent-separated form (see $K(L_C)^+$, Chart 1A).

Chart 1.[a]

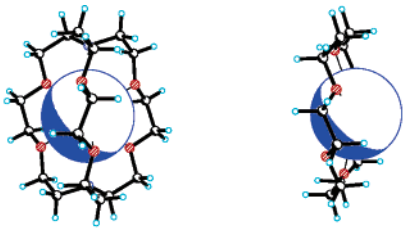

A. $K(L_C)^+$ for "separated" B. $K(L_E)^+$ for "contact"

[a] Note these space-filling representations of potassium cation show how (A) its entombment by [2.2.2]cryptand effectively precludes direct interionic contact and (B) its nesting in 18-crown-6 fully shields only the back face.

By analogous reasoning, the [1:1] complexation of K^+ with the two-dimensional macrocyclic polyether (18-crown-6)[20] is sufficient to protect only the back face of the complexed cation which is then free to form the contact ion pair with nitrobenzenide anion from the unprotected front face (see $K(L_E)^+$, Chart 1B).

The properties of such well-defined separated ion pairs (SIP) and contact ion pairs (CIP) as crystalline salts now provide the opportunity to examine the intrinsic characteristics of various other reactive anions, as they are affected by the countercation in the solid state and in solution, and, hence, their chemical reactivity.[21] To this end, the one-electron reduction of nitroarenes is an especially fortunate choice, since the electronic structure of the resulting anion radical can also be simultaneously probed by ESR in combination with IR and UV−vis spectroscopy. Accordingly, we focus here on various crystalline ion-pair salts derived from *p*-dinitrobenzene reduction to establish the direct relationship between solid-state (X-ray) structures of SIPs and CIPs with those responsible for the ESR and electronic

(7) (a) Nelsen, S. F.; Adamus, J.; Wolff, J. J. *J. Am. Chem. Soc.* **1994**, *116*, 1589. (b) Nelsen, S. F.; Trieber, D. A.; Wolff, J. J.; Powell, D. R.; Rogers-Crowley, S. *J. Am. Chem. Soc.* **1997**, *119*, 6873. (c) Nelsen, S. F.; Ismagilov, R. F.; Powell, D. R. *J. Am. Chem. Soc.* **1997**, *119*, 10213. (d) Nelsen, S. F.; Tran, H. Q.; Nagy, M. A. *J. Am. Chem. Soc.* **1998**, *120*, 298. (e) Nelsen, S. F.; Ismagilov, R. F.; Powell, D. R. *J. Am. Chem. Soc.* **1998**, *120*, 1924. (f) Nelsen, S. F.; Newton, M. D. *J. Phys. Chem. A* **2000**, *104*, 10023.

(8) (a) Marcus, R. A. *J. Phys. Chem. B* **1998**, *102*, 10071. (b) Chen, P.; Meyer, T. J. *Chem. Rev.* **1998**, *98*, 1439. (c) Nelsen, S. F.; Ismagilov, R. F. *J. Phys. Chem. A* **1999**, *103*, 5373. (d) Piotrowiak, P.; Miller, J. R. *J. Phys. Chem.* **1993**, *97*, 13052. (e) Vakarin, E. V.; Holovko, M. F.; Piotrowiak, P. *Chem. Phys. Lett.* **2002**, *363*, 7.

(9) (a) Lambert, C.; Nöll, G. *J. Am. Chem. Soc.* **1999**, *121*, 8434. (b) Coropceanu, V.; Lambert, C.; Noll, G.; Brédas, J. L. *Chem. Phys. Lett.* **2003**, *373*, 153. (c) Szeghalmi, A. V.; Erdmann, M.; Engel, V.; Schmitt, M.; Amthor, S.; Kriegisch, V.; Nöll, G.; Stahl, R.; Lambert, C.; Leusser, D.; Stalke, D.; Zabel, M.; Popp, J. *J. Am. Chem. Soc.* **2004**, *126*, 7834. (d) Nishiumi, T.; Nomura, Y.; Chimoto, Y.; Higuchi, M.; Yamamoto, K. *J. Phys. Chem.* **2004**, *108*, 7992. (e) Nelsen, S. F. *Chem.—Eur. J.* **2000**, *6*, 581. (f) Lindeman, S. V.; Rosokha, S. V.; Sun, D.-L.; Kochi, J. K. *J. Am. Chem. Soc.* **2002**, *124*, 843. (g) Coropceanu, V.; Malagoli, M.; Andre, J. M.; Brédas, J. L. *J. Am. Chem. Soc.* **2002**, *124*, 10519.

(10) Oakes, J.; Slater, J.; Symons, M. C. R. *Trans. Faraday Soc.* **1970**, *66*, 546.

(11) (a) Maki, A. H.; Geske, D. H. *J. Chem. Phys.* **1960**, *33*, 825. (b) Freed, J. H.; Fraenkel, G. K. *J. Chem. Phys.* **1964**, *40*, 1815. (c) Gulick, W. M., Jr.; Geiger, W. E.; Geske, D. H. *J. Am. Chem. Soc.* **1968**, *90*, 4218 (d) Parrish, R. G.; Hall, G. S.; Gulick, W. M. *Mol. Phys.* **1973**, *26*, 1121. (e) Ludwig, P.; Layloff, T.; Adams, R. N. *J. Am. Chem. Soc.* **1964**, *86*, 4568.

(12) Ward, R. L. *J. Am. Chem. Soc.* **1961**, *83*, 1296.

(13) Nelsen, S. F.; Konradsson, A. E.; Weaver, M. N.; Telo, J. P. *J. Am. Chem. Soc.* **2003**, *125*, 12493.

(14) (a) Blandamer, M. J.; Gross, J. M.; Symons, M. C. R. *Nature* **1965**, *205* (4971), 591. (b) Gross, J. M.; Symons, M. C. R. *Mol. Phys.* **1965**, *9*, 287. (c) Gross, J. M.; Symons, M. C. R. *Trans. Faraday Soc.* **1967**, *63*, 2117. (d) Oakes, J.; Symons, M. C. R. *Chem. Commun.* **1968**, 294.

(15) (a) Szwarc, M., Ed. *Ions and Ion Pairs in Organic Reactions*; Wiley-Interscience: New York, 1972; Vols. 1 and 2. (b) Streitwieser, A., Jr. *Solvolytic Displacement Reactions*; McGraw-Hill: New York, 1962. (c) Gordon, J. E. *Organic Chemistry of Electrolyte Solutions*; Wiley: New York, 1975. (d) Thermodynamics (and kinetics) justification for two principal types of such dynamic ion pairs is presented by Szwarc in ref 15a.

(16) Davlieva, M. G.; Lü, J. M.; Lindeman, S. V.; Kochi, J. K. *J. Am. Chem. Soc.* **2004**, *126*, 4557.

(17) (a) Our operational classification of the *contact* ion pair herein requires direct interionic contact between the positive and negative centers (within their van der Waals radii). By contrast, such a direct electrostatic interaction between cation/anion centers is modified in the *separated* ion pair by intervention of one or more solvent, ligand, etc. (b) The absence of close contacts (less than van der Waals separation) between the crown-ethers (or cryptand) and dinitrobenzenide indicates that there are no special (bonding) interactions of the anion with the ligand(s).

(18) For representative examples of isolated ion pairs of aromatic anion radicals via alkali-metal reductions, see: (a) Mooij, J. J.; Klaassen, A. A. K.; de Boer, E.; Degens, H. M. L.; van der Hark, T. E. M.; Noordik, J. H. *J. Am. Chem. Soc.* **1976**, *98*, 680. (b) Jost, W.; Adam, M.; Enkelmann, V.; Muellen, K. *Angew. Chem., Int. Ed. Engl.* **1992**, *31*, 878. (c) Janiak, C.; Hemling, H. *Chem. Ber.* **1994**, *127*, 1251. (d) Bock, H.; Arad, C.; Naether, C.; Havlas, Z. *Chem. Commun.* **1995**, 2393. (e) Naether, C.; Bock, H.; Claridge, R. F. C. *Helv. Chim. Acta* **1996**, *79*, 84. (f) Naether, C.; Bock, H.; Havlas, Z.; Hauck, T. *Organometallics* **1998**, *17*, 4707. (g) Bock, H.; Gharagozloo-Hubmann, K.; Slevert, M.; Prisner, T.; Havlas, Z. *Nature* **2000**, *404*, 267. (h) Hitchcock, P. B.; Lappert, M. F.; Protchenko, A. V. *J. Am. Chem. Soc.* **2001**, *123*, 189.

(19) Dietrich, B.; Lehn, J. M.; Sauvage, J. P.; Blanzat, J. *Tetrahedron* **1973**, *29*, 1629.

(20) Cram, D. J.; Trueblood, K. N. *Top. Curr. Chem.* **1981**, *98*, 43.

(21) (a) Loupy, A.; Tchoubar, B. *Effets des Sales en Chimie Organque et Organometallique*; Dunod University: Paris, 1988. (b) Kosower, E. M. *Introduction to Physical Organic Chemistry*; Wiley: New York, 1968. (c) Kaiser, E. T.; Kevan, L. *Radical Ions*; Interscience: New York, 1968. (d) Peters, S. J.; Turk, M. R.; Kiesewetter, M. K.; Reiter, R. C.; Stevenson, C. D. *J. Am. Chem. Soc.* **2003**, *125*, 11212. (e) Batz, M. L.; Garland, P. M.; Reiter, R. C.; Sandborn, M. D.; Stevenson, C. D. *J. Org. Chem.* **1997**, *62*, 2045.

Chart 2

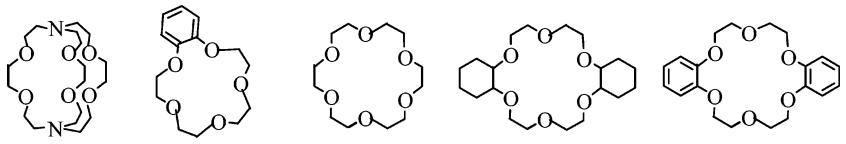

L_C L_{E1} L_{E2} L_{E3} L_{E4}

Table 1. Principal Geometric Parameters of Dinitrobenzenide (DNB^-) in Crystalline Ion-Pair Salts

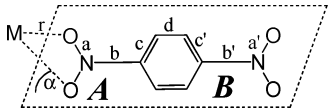

		α,[a] deg	β,[b] deg	*r*, Å	*a*, Å	*b*, Å	*c*, Å	*d*, Å
				a. Separated Ion-Pair Salt				
$K(L_C)^+//DNB^-$	***A*-NO_2**		2.8	4.821(1)	1.259(1)	1.403(1)	1.409(1)	1.372(1)
	***B*-NO_2**		2.9	5.150(1)	1.260(1)	1.408(1)	1.409(1)	
$K(L_{E1})_2^+//DNB^-$	***A*-NO_2**		3.7	5.339(1)	1.255(1)	1.406(2)	1.407(1)	1.372(1)
	***B*-NO_2**		2.0	6.312(1)	1.255(1)	1.407(2)	1.408(1)	
				b. Contact Ion-Pair Salt				
$K(L_{E3})^+DNB^-$	***A*-NO_2**	37.4	1.4	3.191(3)	1.247(3)	1.384(4)	1.398(4)	1.359(3)
		47.3	1.3	2.699(3)	1.277(3)		1.412(4)	
	***B*-NO_2**		0.2	5.703(3)	1.251(3)	1.408(4)	1.400(4)	
			−0.5	7.461(3)	1.246(3)		1.397(4)	
				c. Contact Dianion Triple Salt				
$[K(L_{E2})^+]_2DNB^{2-}$	***A*-NO_2**	6.7	1.8	2.737(1)	1.296(2)	1.353(4)	1.434(3)	1.357(3)
	***B*-NO_2**	5.5	5.4	2.747(1)	1.304(2)	1.346(4)	1.431(3)	
				d. Neutral Acceptor				
DNB[c]			10.2		1.228	1.470	1.390	1.391

[a] α is the out-of-plane angle of the K−O bond. [b] β is the torsion angle O−N−C−C. [c] Data from Cambridge Structural Database (ref. DNITBZ02).

(UV−vis) spectra in solution, especially insofar as the accompanying electronic changes in dinitrobenzenide as a mixed-valence anion.

Results

I. Isolation of Dinitrobenzenide Anion as Crystalline Ion-Pair Salts. The successful preparation of pure ion-pair salts was critically dependent on the presence of the polyether ligands depicted in Chart 2 during the potassium-mirror reduction of *p*-dinitrobenzene in THF solution (see Experimental Section for synthetic details).

"Separated" ion-pair salts of dinitrobenzene anion radical obtained when the coordination sites of K^+ were fully saturated by the presence of either (a) 1 equiv of [2,2,2] cryptand as the complexed cation $K(L_C)^+$ or (b) 2 equiv of the crown-ether ligand benzo-15-crown-5 as $K(L_{E1})_2^+$ to simultaneously protect both its back face and its front face.

"Contact" ion-pair salts were generally more labile than the corresponding SIP salt, and we were able to isolate only the [1:1] dicyclohexano-18-crown-6 (L_{E3}) complex with K^+ as a single-crystal suitable for X-ray crystallography (Table 1). Repeated attempts to utilize the other 18-crown-6 ligands, L_{E2} and L_{E4}, afforded contact ion-pair salts that were crystalline and useful for UV−vis spectral measurements (vide infra) but unsuited for X-ray analysis.[22] Interestingly, the smaller macrocyclic benzo-15-crown-5 ligand L_{E1} consistently afforded only the bis-complex $K(L_{E1})_2^+$ as the separated ion pair (vide supra) - - even during crystallization from THF solutions containing a large deficit of the ligand (relative to K^+).

The ternary ion-triplet salt of the diamagnetic *p*-dinitrobenzene dianion (DNB^{2-}) was prepared as the "contact" complex consisting of the [2:1] salt/$[K(L_{E2})^+]_2(DNB^{2-})$ via the low-temperature reduction of *p*-dinitrobenzene in the presence of potassium mirror and the 18-crown-6 ligand, both in excess. Unfortunately, we were not able to isolate the separated ion triplet based on the [2,2,2]cryptand ligand largely owing to the insolubility of the separated ion-pair salt.

II. X-ray Crystallography of Pure Dinitrobenzenide Salts. A. Ligated Potassium Salts as Crystalline "Separated" Ion Pairs. The diffraction data of highly hygroscopic dark green plates of the cryptand complex $K(L_C)^+//DNB^{-\bullet}$ were collected at −150 °C, and the crystal structure was solved and refined by conventional methods (see Experimental Section) to a uniform precision of 0.2−0.4 pm. A cursory glance of the packing pattern in the monoclinic unit cell illustrated in Figure 1A quickly establishes the "separated" dinitrobenzenide anion to exist as an independent entity apart from its potassium counterion as the cryptand complex $K(L_C)^+$. Indeed, even the interionic separation of potassium from the nearest NO_2-center of neighboring DNB anions (arbitrary taken as the K....O distance) with $r > 4.8$ Å is significantly larger than the sum of their van der Waals radii (4.3 Å). The same general picture emerges from the packing observed in the triclinic unit cell of the bis-benzo-15-crown-5 complex of potassium $K(L_{E1})_2^+//DNB^{-\bullet}$ shown in Figure 1B, and the interionic separation of $r > 5$ Å is even

(22) The related dibenzo-18-crown-6 ligand L_{E4} afforded from various solutions only microscopic polycrystalline materials that were pure but unsuitable for X-ray analysis even after repeated attempts. Likewise, the parent 18-crown-6 ligand L_{E2} led to very thin plates.

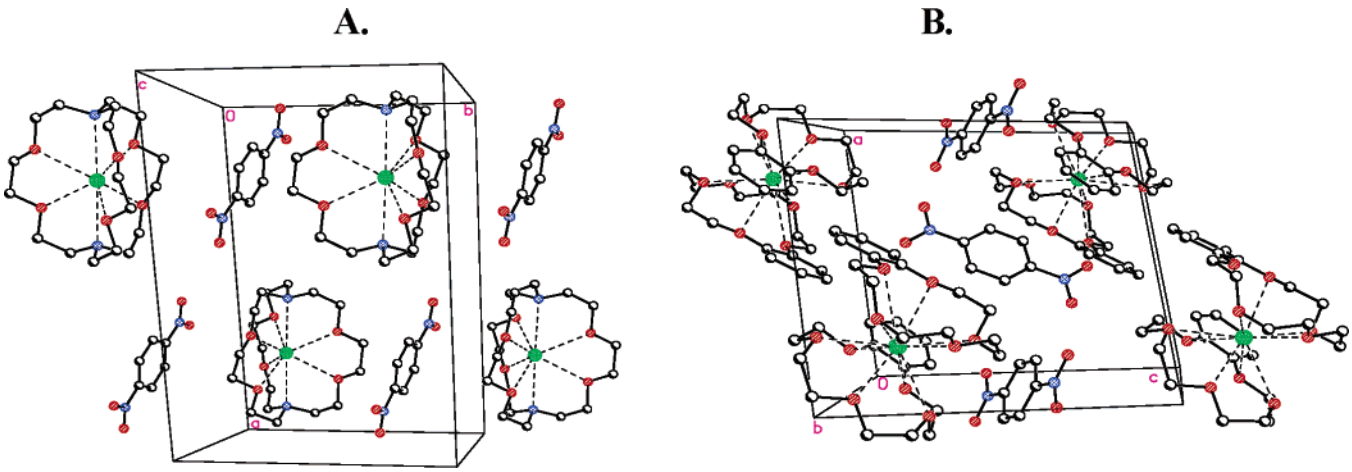

Figure 1. Unit cells of "separated" ion-pair salts: K $(L_C)^+$//DNB^- (A) and $K(L_{E1})_2^+$//DNB^- (B) showing the packings of loosely associated cation/anion pairs, each as discrete entities.

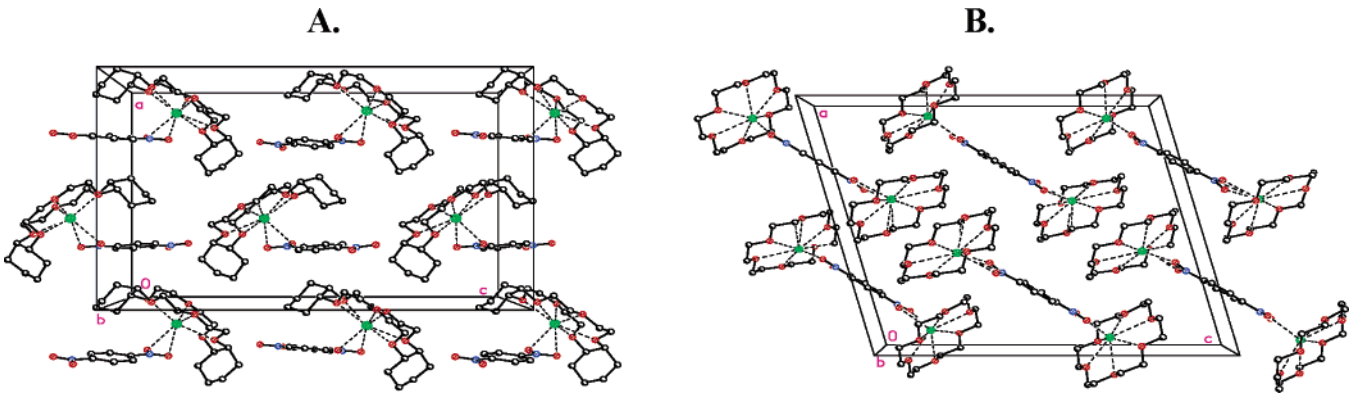

Figure 2. Unit cells of the "contact" ion-pair $K(L_{E3})^+DNB^-$ (A) and "contact" ion triplet $[K(L_{E2})^+]_2DNB^{2-}$ (B) showing the tight association of cation/anion pairs as indistinguishable entities.

larger than that in the cryptand complex. Both unit cells in Figure 1 consist of close-packed quasi-spherical cations in which the voids are occupied by individual dinitrobenzenide anions, and an anionic NO_2-center thus lies within van der Waals distance of the outer lipophilic (cryptand or crown-ether) sheath of K^+.[17b] Such loose structures therefore represent true crystalline forms of what have been qualitatively described as "solvent-separated" ion pairs in solution.[15]

B. Crystalline Dinitrobenzenide Salts as the "Contact" Ion Pair and the Ion Triplet. A labile dark green needle of the dinitrobenzenide salt of the dicyclohexano-18-crown-6 complex $K(L_{E3})^+$ was successfully mounted at −100 °C, and Figure 2A shows the packing pattern in the orthorhombic unit cell to consist of only a *single* type of tight ion-pair assembly. The interionic separation between K^+ and DNB^- is quite intimate and highly unsymmetrical in two ways. First, the two nitro groups in DNB^- are markedly nonequivalent, with one NO_2-center (A) tightly bonded with a very close K^+....O contact of $r_1 = 2.7$ Å, whereas the other NO_2-center (B) is nonbonded with $r_B > 10$ Å. Second, NO_2-center A is unsymmetrically bonded to potassium, with the second oxygen showing a longer K^+....O contact of $r_2 = 3.2$ Å. As such, this tight and unsymmetrical binding of the crown ether-ligated cation to only a single nitro-center is generally in the form that is somewhat reminiscent of covalent bonding in other σ-complexes.[23] As such, the direct coordination of the crown ether-ligated K^+ via its free front face (compare $K(L_E)^+$ in Chart 1) to dinitrobenzenide then constitutes the crystalline counterpart of the "contact" ion pair in solution.

The packing pattern in the monoclinic unit cell of the dark yellow plate of the ternary dianion salt in Figure 2B also shows the presence of only a single tightly bound ionic assembly of $[K(L_{E2})^+]_2DNB^{2-}$. Thus, both NO_2-centers of the dinitrobenzenide dianion are very close to a pair of complexed cations $K(18\text{-crown-}6)^+$ via their open front face (see Chart 1B). The short interionic separation of $r \approx 2.7$ Å in Table 1 is diagnostic of contact ion pairing generally in the symmetric bidentate form, (more or less) related to that in the monoanion salt described above.

III. Optical Transitions in "Separated" and "Contact" Ion Pairs from Dinitrobenzenide Anions in Solution and in the Crystalline Solid State. A. Electronic Spectra in Solution. Dissolution of the crystalline ion-pair salts of dinitrobenzenide anion in Table 1 afforded yellow-green to green THF solutions which consistently showed two groups of diagnostic absorption bands in the UV−vis spectra (Table 2). The high-energy envelope (I) with $\lambda_{max} \approx 400$ nm was singularly invariant with

(23) For other examples of similar bonding of crown ether-ligated potassium, see: (a) Caswell, L. R.; Hardcastle, J. E.; Jordan, T. A.; Alam, I.; McDowell, K. A.; Mahan, C. A.; Fronczek, F. R.; Gandour R. D. *J. Inclusion Phenom. Macrocyclic Chem.* **1992**, *13*, 37. (b) Veya, P.; Floriani, C.; Chiesi-Villa, A.; Rizzoli, C. *Organometallics* **1994**, *13*, 214. (c) Mlinaric-Majerski, K.; Visnjevac, A.; Kragol, G.; Kojic-Prodic, B. *J. Mol. Struct.* **2000**, *554*, 279. (d) Dyer, R. B.; Ghirardelli, R. G.; Palmer, R. A.; Holt, E. M *Inorg. Chem.* **1986**, *25*, 3184. (e) See also: Cambillau, C.; Bram, G.; Corset, J.; Riche, C. *Can. J. Chem.* **1982**, *60*, 2554.

Table 2. Electronic Absorption Spectra of Dinitrobenzenide Ion-Paired with Complexed K^{+a}

	$\lambda_{max}(\epsilon)$	
$K(L)^+$	envelope I	envelope II
$K(L_C)^+$	396 (6.7) 420 (6.0)	800 (7.0) 835 (8.8) 915 (21)
$K(L_{E4})^+$	400 (5.4) 420(5.4)	772sh 847 (7.0) 910(4.0)
$K(L_{E3})^{+\,c}$	396 (6.3) 420sh	800(7.7) 832sh 855(9.1) 910(11)
K^{+d}	400 420	764 847 911

[a] In THF, at 20 °C, unless noted otherwise; λ_{max}, in nm, ϵ in 10^3 M^{-1} cm^{-1}. [b] Spectral characteristics are the same for $K(L_{E1})_2^+//DNB^{-\bullet}$. [c] Spectral characteristics are the same for $K(L_{E2})^+DNB^{-\bullet}$. [d] DME solution.

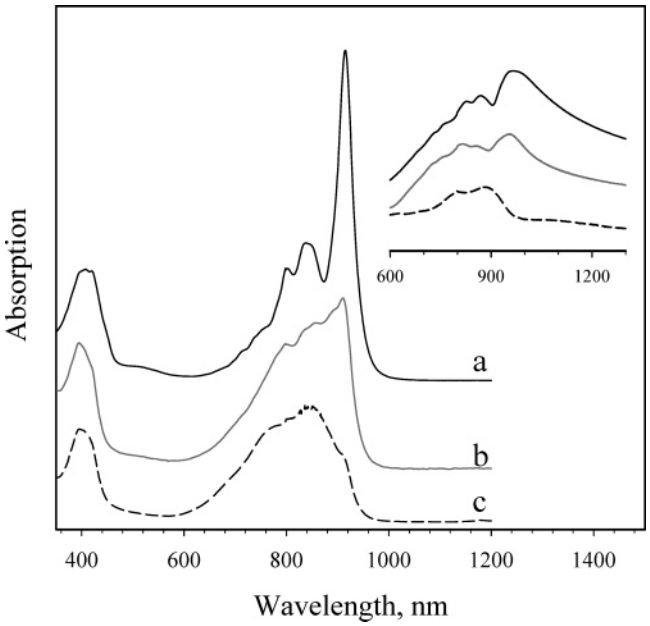

Figure 3. UV−NIR spectra of ion-pair salts dissolved into THF (20 °C): (a) $K(L_C)^+$ //DNB^-, (b) $K(L_{E3})^+DNB^-$, and (c) $K(L_{E4})^+DNB^-$. Inset: corresponding solid-state spectra of crystalline salts suspended in mineral oil (see text).

the changes in both the complexed K^+ counterion and the temperature. Moreover, the similarity of envelope I (though slightly blue-shifted) to that observed in the parent nitrobenzenide anion (NB^-) indicated that it derives from local transitions associated with the negatively charged nitroarene chromophore. By way of contrast, the second, low-energy envelope II in the near-IR region (650−950 nm and not present in NB^-) was both cation- and temperature-dependent as follows.

The UV−vis spectrum in Figure 3a obtained from the dissolution of the crystalline cryptand salt $K(L_C)^+//DNB^-$ into THF was quite similar but slightly blue-shifted relative to dinitrobenzenide anion previously generated in situ via the sodium-amalgam reduction of *p*-dinitrobenzene together with [2,2,2]cryptand in DMF solution.[24] Particularly relevant in Figure 3a is the decreasing progression of resolved bands assigned to splitting into vibronic components of the intramolecular charge-transfer (intervalence) transition (vide infra).[13] Since the identical spectrum was also observed upon dissolution of the [2:1] complex of benzo-15-crown-5 with K^+ as the crystalline salt $K(L_{E1})_2^+DNB^-$, it is easy to conclude that spectrum 3a represents dinitrobenzenide anion in the separated ion-pair form, independent of whether K^+ is complexed to cryptand or two benzo-15-crown-5 ligands. Moreover, the similarity of Figure 3a to the spectrum in the more polar solvent (DMF)[13] strongly suggests that it is spectrally indistinguishable from that of free dinitrobenzenide anion in solution.

Dissolution of the dicyclohexano-18-crown-6 complex as the crystalline contact ion-pair salt $K(L_{E3})^+DNB^-$ into THF afforded the UV−vis spectrum in Figure 3b showing partially resolved envelope II to resemble that in Figure 3a, but with the marked attenuation of the lowest energy vibronic band from $\lambda_{max} = 915$ nm (ϵ 21 000 M^{-1} cm^{-1}) to $\lambda_{max} = 910$ nm (ϵ 11 000 M^{-1} cm^{-1}). Essentially the same unique spectral progression was observed in THF solutions resulting from the dissolution of the crystalline 18-crown-6 complex $K(L_{E2})^+DNB^-$.

Finally, the solution spectrum obtained from the crystalline dibenzo-18-crown-6 complex $K(L_{E4})^+DNB^-$, as shown in Figure 3c, is quite unique in that the lowest energy vibronic component in envelope II is almost missing in Figure 3c, merely showing up as a weak shoulder at $\lambda_{sh} = 910$ nm.

B. Electronic Spectra in the Solid State. The diagnostic intervalence transitions (envelope II) of crystalline ion pairs are isolated in the inset of Figure 3. The three solid-state spectra corresponding to the solution spectra of the prototypical salts were taken as extremely hygroscopic powders finely suspended in mineral oil and measured in absorption mode.[25]

Barring some minor complications from reflective dispersion as well as crystal lattice effects, the solid-state spectra show considerable resolution, certainly sufficient to observe the retention of fine-structure characteristics in common with those in the solution spectra. Most importantly, such an unambiguous spectral correspondence establishes the direct structural relationship between the separated and contact ion pairs measured as dynamic species in solution vis á vis those defined by X-ray analysis in the crystalline solid state.[23e]

IV. ESR Spectra of Dinitrobenzene Anion Radicals and the Temperature-Dependent Dynamics of "Separated" and "Contact" Ion Pairs. A. Hyperfine Differentiation in Static ESR Spectra of Dinitrobenzenide Ion Pairs. Dissolution of the crystalline dinitrobenzenide salts of K^+ complexed to cryptand and to two benzo-15-crown-5 ligands as the separated ion pairs salts $K(L_C)^+//DNB^-$ and $K(L_{E1})_2^+//DNB^-$, respectively, into THF solvent afforded identical ESR spectra (Figure 4a) that are characterized by well-resolved hyperfine splittings from two nitrogens and four hydrogens (Table 3). This ESR spectrum was temperature-independent over the range 170−300 K, and it thus corresponds to a static $DNB^{-\bullet}$ structure (on the ESR time scale of $>10^{-8}$s) showing delocalization of the unpaired electron between two equivalent NO_2-centers, as expected from a symmetrical $DNB^{-\bullet}$ structure unencumbered by its counterion, i.e., a "separated" ion pair.[26]

By way of contrast, dissolution of the crystalline dibenzo-18-crown-6 complex as the contact ion-pair salt $K(L_{E4})^+DNB^-$

(24) For comparison, free nitrobenzenide prepared in situ in DMF by Nelsen and co-workers[13] was characterized by an intervalence (NIR) absorption with maxima at 924 (20.3), 851 (11.9), and 815 (10.3) (in nm, in parentheses; extinction coefficients, in 10^3 M^{-1} cm^{-1}).

(25) (a) Essentially the same spectra (although broadened) were obtained in Al_2O_3 matrixes measured in the reflectance mode. (b) Note that dinitrobenzenide salts are insoluble in hydrocarbon solvents and, thus, precludes their dissolution in the mineral oil used in this study. Therefore, the spectra of dinitrobenzenide anion salts finely ground in mineral oil (presented in the inset of Figure 3) represent that of the pure solid state.

(26) (a) It is to be noted that the hyperfine splittings in Table 3 are significantly less than $a_{2N} = 1.74$ G and $a_{4H} = 1.12$ G reported earlier for "delocalized" *p*-dinitrobenzene anion radical generated electrochemically in the presence of alkylammonium counterions.[11a] (b) Note that all ion-pair salts show broad (unresolved) solid-state ESR spectra, even when very finely ground.

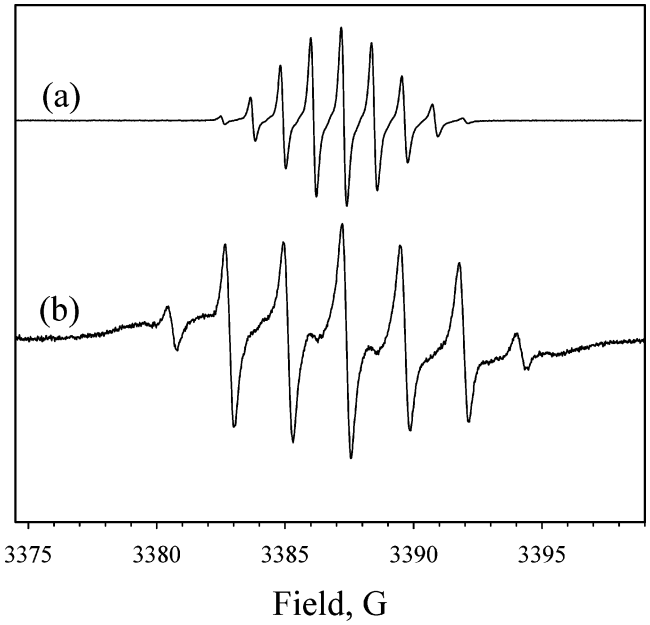

Figure 4. ESR spectra of crystalline ion pairs dissolved into THF as the (a) "separated" $K(L_C)^+$//DNB^- showing hyperfine splittings a_{2N} and a_{4H} and (b) "contact" $K(L_{E4})^+DNB^-$ showing splittings a_{1N} and a_{2H} at 293 K.

Table 3. ESR Hyperfine Splittings (G) of Dinitrobenzene Anion Radicals Ion-Paired with Complexed K^+[a]

$K(L)^+$	a_N	a_H
$K(L_C)^+$	1.23 (2N)	1.11 (4H)
$K(L_{E1})_2^+$	1.23 (2N)	1.11 (4H)
$K(L_{E4})^+$	4.56 (1N)[b]	2.30 (2H)[b]
	5.0 (1N), 0.4 (1N)[c]	2.5 (2H)[c]
$K(L_{E2})^+$[d]	3.3 (1N)[e]	~0.2 (2D)
$K(L_{E3})^+$[d]	3.2(1N)[e]	~0.2 (2D)

[a] In THF. [b] CIP_1. [c] CIP_2. [d] DNB-d_4^-. [e] At room temperature, the spectra are doubled due to intramolecular self-exchange (see text).

into THF at 313 K showed a narrow-line ESR spectrum (Figure 4b) with hyperfine splittings to only a single nitrogen (a_N = 4.56 G) and two hydrogens (a_{2H} = 2.30 G) that correspond to electron localization only to a single NO_2-center, as expected from a unsymmetrical $DNB^{-\bullet}$ structure with intimate K^+ association to one NO_2-center, i.e., a "contact" ion pair.

B. Temperature-Dependent Hyperfine Splittings of Dinitrobenzenide Ion Pairs. The ESR spectra of contact ion-pair salts dissolved in THF showed two types of temperature-dependent behavior that are nominally classified as (i) increases in the number of resolved hyperfine splittings and (ii) selective line broadening of the hyperfine lines that are indicative of thermodynamic equilibria and dynamic rate processes as follows.

(i) Thermodynamic equilibria between contact ion pairs are best illustrated by following the temperature-dependent ESR spectrum of the dibenzo-18-crown-6 complex $K(L_{E4})^+DNB^-$ shown in Figure 4b.[27a] The series of ESR spectra of this contact ion pair in THF solution (Figure 5) show the gradual appearance of new species that are first noticeable at 273 K and progressively increase in intensity (at the expense of original spectrum)

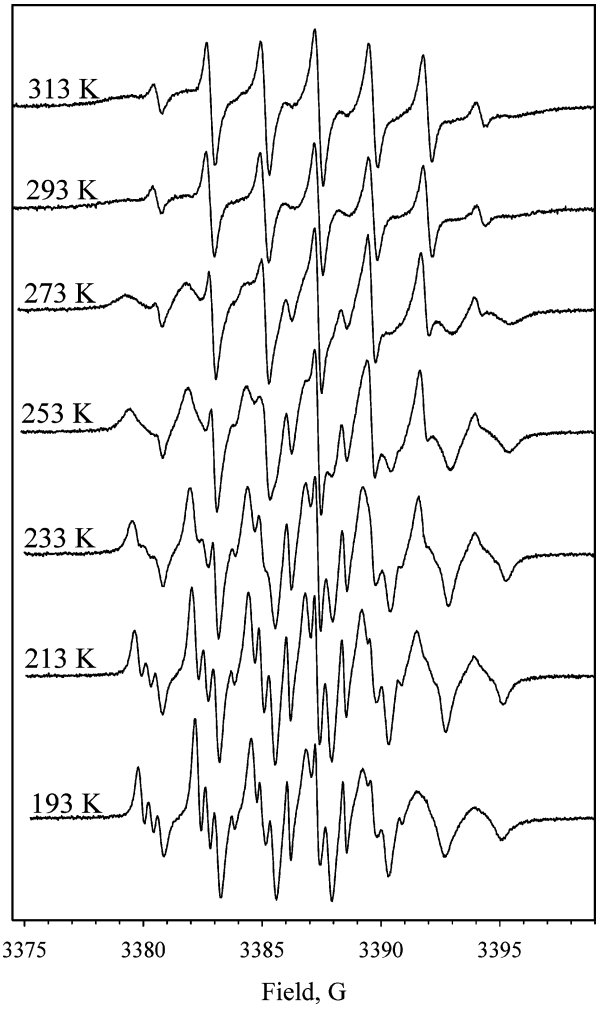

Figure 5. Temperature-dependent ESR spectrum of crystalline $K(L_{E4})^+DNB^-$ dissolved into THF showing equilibria between CIP_1 and CIP_2 with SIP in eq 2. The 313 K spectrum corresponds to CIP_1, and lowering the temperature leads to increasing fraction of CIP_2 with broader lines. Note the appearance of SIP at lowest temperature.

as the temperature is lowered.[27b] Such a spectral change is consistent with the relatively straightforward conversion of the high-temperature species with hyperfine lines (a_N = 4.56 G, a_{2H} = 2.30 G) to a somewhat similar species with hyperfine lines (a_N = 5.0 G, a_{2H} = 2.5 G) that is prominent at <213 K. Since this spectral change is reversible, it is reasonable to include the existence of a temperature-dependent equilibrium between a pair of isomeric contact ion pairs, i.e.,

$$CIP_1 \overset{K_{iso}}{\rightleftharpoons} CIP_2 \qquad (1)$$

Deconvolution of a composite spectrum leads to the isomerization constant in eq 1 K_{iso} = 5 at 293 K and the thermodynamic parameters $\Delta H_{iso} = -1.5$ kcal mol^{-1} and $\Delta S_{iso} = -2$ eu in the temperature range 223−313 K (Figure S1 in Supporting Information). Finally, at the lowest practicable temperature of 193 K, a small spectral admixture of a third species with hyperfine splittings of a_{2N} =1.23 G (the same as those observed in Figure 4a) indicated further solvent separation, i.e.,

$$CIP_1 \overset{K_{iso}}{\rightleftharpoons} CIP_2 \overset{K_{sep}}{\rightleftharpoons} SIP \qquad (2)$$

which is estimated to be ~5% at the lowest temperature studied.[28]

(27) (a) The peak-to-peak line widths ($\Delta H \approx 0.3$ G) in the ESR spectra of species 1 were invariant between 253 and 313 K. (b) The line width of species 2 was significantly broader ($\Delta H \approx 1.3$ G at 293 K) than that of species 1 and slightly temperature-dependent.

(28) (a) Based on earlier ESR studies, the enthalpy change (ΔH) in the CIP-to-SIP interconversion is negative. See: (b) Hirota, N. *J. Phys. Chem.* **1967**, *71*, 127.

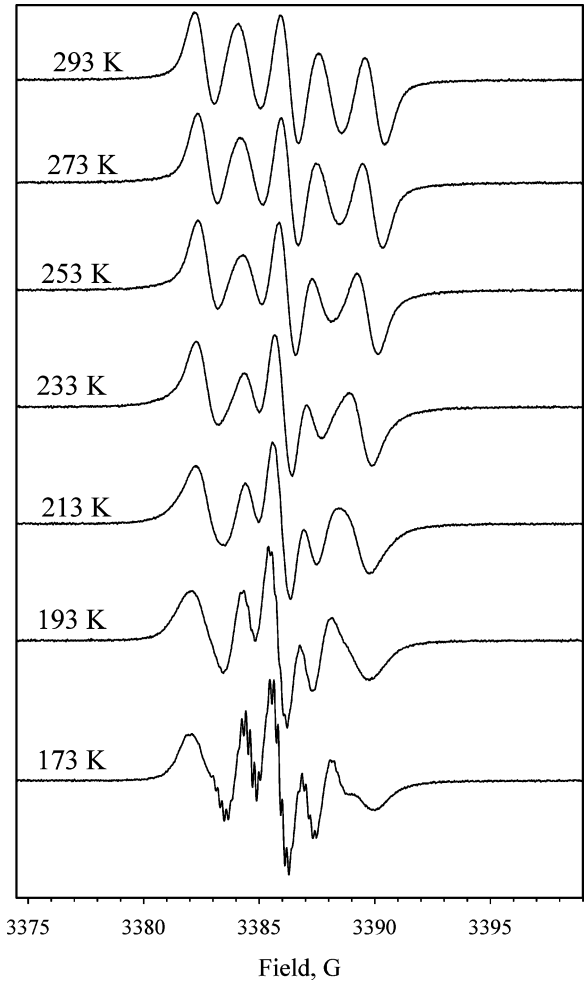

Figure 6. Temperature-dependent ESR spectrum of $K(L_{E3})^+DNB\text{-}d_4^-$ showing ion-pair exchange (eq 3) of CIP_3 that leads to SIP at the lowest temperature (see text).

(ii) Interchange dynamics of contact ion pairs are readily evaluated in the temperature-dependent ESR spectrum of the crystalline salt of the dicyclohexano-18-crown-6 complex $K(L_{E3})^+DNB^-$ dissolved into THF. Since the temperature-dependent ESR spectral changes of this salt (Figure S2) were difficult to decipher quantitatively, dinitrobenzene was converted to the perdeuterated derivative (DNB-d_4, as described in the Experimental Section). Indeed, deuterium substitution simplified the picture considerably, and the ESR spectrum of $K(L_{E3})^+$-DNB-d_4^- showed five major lines at 293 K (Figure 6). At first glance, such an ESR spectrum might be assigned to a species with the spin delocalized over two nitrogens. However, the progressive lowering of the temperature resulted in the selective broadening and gradual disappearance of two lines with $m_I = \pm 1$, so at low temperature (213 K) the ESR spectrum consisted predominantly of a three-line (1:1:1) splitting with $a_N = 3.3$ G. Quantitative line broadening analysis[29] of the high-temperature spectra, particularly in the range 233−293 K, reproduced this alternating line width broadening (see Figure S3 in Supporting Information) arising from the contact ion pair with $a_N = 3.3$ G.

(29) Heinzer, J. Quantum Chemistry Program Exchange 209, as modified by Petillo, P. A. and Ismagilov, R. F. We thank Prof. S. F. Nelsen for kindly providing us with a copy of this program.

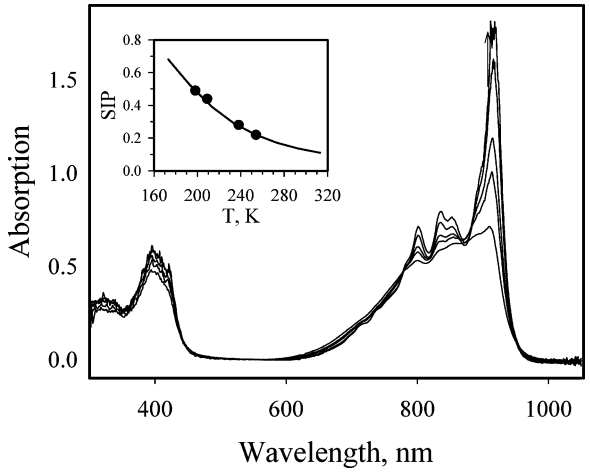

Figure 7. Temperature-dependence of the UV−NIR spectrum of $K(L_{E3})^+DNB^-$ in THF measured at (bottom-to-top) 295, 259, 233, 213, and 190 K to reflect the SIP ⇄ CIP interchange in eq 4. Inset: fraction of SIP fitted with $\Delta H = -3.6$ kcal/mol and $\Delta S = -20$ eu.

Such a dynamic behavior can be related to intramolecular spin-exchange between two different NO_2-centers in the contact ion pair, e.g.,

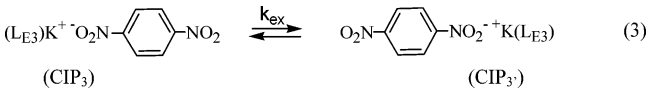

(3)

Stated alternatively, the exchange in eq 3 can be sufficiently slow at low temperature to generate the static ESR spectrum of the "frozen" contact ion pair. With rising temperatures, the interchange rate increases and leads to the doubling of the ESR spectra (apparent in the 293 K spectrum). Dynamic ESR simulation (Figure S3) of such a self-exchange between two NO_2-centers in *p*-dinitrobenzene anion radical that is closely paired to $K(L_{E3})^+$ yields the first-order rate constant $k_{ex} = 8 \times 10^8$ s^{-1} at 293 K with the activation barrier $\Delta H^{\neq}_{ex} = 0.8$ kcal/mol and $\Delta S^{\neq}_{ex} = -5$ eu. Finally, at the lowest (practicable) temperature of 173 K, additional hyperfine features are apparent in Figure 6 (bottom spectrum) which can be readily assigned to the ESR spectrum ($a_{2N} = 1.23$ G) corresponding to completely delocalized dinitrobenzene anion radical (Figure 4a) in reversible equilibrium with the contact ion pair, i.e.,

$$CIP_3 \overset{k_{ex}}{\rightleftharpoons} CIP_{3'} \overset{K_{sep}}{\rightleftharpoons} SIP \qquad (4)$$

Additional experimental support for such an interconversion of contact and separated ion pairs is obtained independently by observing the temperature-dependent spectral (UV−vis) changes under the same conditions. Thus Figure 7 confirms the spectral interchange of contact and separated ion pairs derived from dicyclohexano-18-crown-6 complex K^+ salt in the temperature range 295−190 K. The inset shows the fit of the spectral data to the equilibrium in eq 4 with $\Delta H_{sep} = -3.6$ kcal/mol and $\Delta S_{sep} = -20$ eu. The preferential formation of this separated ion pair at low temperatures is analogous to that observed with dibenzo-18-crown-6 complexed K^+ in eq 2, but its magnitude is significantly larger, as indicated by comparative deconvolutions of the low-temperature ESR spectra (Figures S4 and S5).

Finally, it is important to note that the temperature-dependent ESR spectra in Figure 6 are essentially identical to those obtained from the related contact ion-pair salt derived from the 18-crown-6 analogue $K(L_{E2})^+DNB\text{-}d_4^-$, as well as those from the undeuterated parent $K(L_{E2})^+DNB^-$ (see Figures S6 and S7, Supporting Information). Moreover, the self-exchange rate $k_{ex} = 10 \times 10^8\ s^{-1}$ at 293 K for the contact ion pair from $(L_{E2})^+$-DNB-d_4^- and activation barrier $\Delta H^{\neq}_{ex} = 0.9$ kcal/mol and $\Delta S^{\neq}_{ex} = -4$ eu in THF solution are the same as those derived from the dicyclohexano-18-crown-6 complex (vide supra). The latter underscores the fact that spectral measurements can provide ready diagnostic probes for precisely distinguishing various ion pairs that are structurally defined by the counterion, even in solution.

Discussion

The clear differentiation of ion-pair structures, particularly in those aspects relevant to "separated" and "contact" in Figures 1 and 2, respectively, represents the unambiguous starting point for their structural comparison with dynamic species extant in solution, as deduced from less definitive (indirect) spectral methods. Accordingly, let us first scrutinize our X-ray data and glean from the precise interatomic distances and angles the quantitative changes in dinitrobenzenide moieties attendant upon formation of different ion pairs.

I. X-ray Structure Analysis: Charge Delocalization and Electronic Coupling of NO_2-Centers in Dinitrobenzenide Ion Pairs. The X-ray parameters in Table 1 (entries 1 and 2) establish the dinitrobenzenide moiety to exist within the separated ion pair as an essentially planar D_{2h}-symmetric anion. Thus, upon one-electron reduction, the neutral *p*-dinitrobenzene acceptor (Table 1, entry 5) undergoes planarization and a symmetric molecular distortion accompanied by elongation of all N−O bonds, marked contraction of both N−C bonds, and elongation of the phenylenyl bridge. Such a highly symmetrical structural change is magnified in dinitrobenzene dianion (Table 1, entry 4) by a factor of roughly 2.[30]

The contrasting formation of the contact ion pair (Table 1, entry 3) is accompanied by the loss of all symmetry elements. Although both NO_2-centers show bond-length increases upon reduction, the change is decidedly unsymmetrical, being more pronounced at the coordinated site. Thus the average value of the two N−O bonds in the latter is slightly longer (closer to that in the dianion) than that in the uncoordinated NO_2-center (closer to that in the neutral acceptor). Furthermore, this unsymmetric distortion also shows up in similar fashion in the C−N bonds that are shorter at the coordinated site and longer at the other C−N bond (both relative to that in the symmetrical "separated" $DNB^{-\bullet}$). In other words, as the result of "contact" ion pairing, the electron-density distribution over the entire dinitrobenzenide moiety is skewed toward the site of the positive charge.

To quantify such inherent differences between separated and contact ion pairs, let us examine the structures of the dinitrobenzenide moiety in terms of (i) selective bond-length/ charge-density distributions, (ii) quinonoidal distortions of the phenylenyl bridge, and (iii) deviations from planarity as follows.

(30) Although "contact" ion pairing pertains to the dianion salt, the bond length changes are sufficiently small to approximate these changes in the "separated" ion triplet.

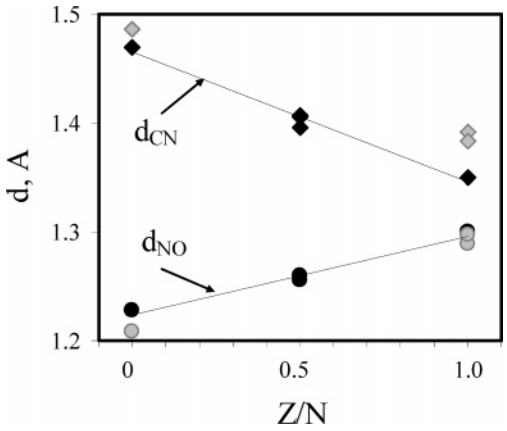

Figure 8. Correlation of the bond length (*d*) with reduced state of acceptor (*Z*/*N*) for comparison to *p*-dinitrobenzene (black) and nitrobenzene (grey). [Note that there are three black overlapping rhombics and three black circles at $Z/N = 0.5$, representing two SIPs and one CIP of $DNB^{-\bullet}$; two gray rhombics and two gray circles at $Z/N = 1$ represent CIP and SIP of $NB^{-\bullet}$.]

Table 4. Estimation of Charge Distribution between Paired NO_2-Centers and Quinonoidal Distortion of the Phenylene Bridge (d_q) in the Dinitrobenzenide Ion Pairs and Dianion Triplet

ion-pair salt	q'/q^a	$d_q{}^b$
$K(L_C)^+DNB^-$	0.5/0.5	0.25 (0.36)
$K(L_{E1})_2{}^+DNB^-$	0.5/0.5	0.25 (0.36)
$K(L_{E3})^+DNB^-$	0.6/0.4[c]	0.32 (0.44)
$[K(L_{E2})^+]_2\,DNB^{2-}$	1.0/1.0	0.52 (0.72)
DNB	0.0/0.0	0.0 (0.0)

[a] Charge on NO_2-center in dinitrobenzenide dianion taken as unity. [b] For quinonoidal distortion, the central C−C bond in benzoquinone is taken as unity; in parentheses, values calculated taking into account the C−N bond changes. [c] Coordinated/noncoordinated NO_2-centers.

(i) The bond length dependence on the effective reduced state of dinitrobenzene can be taken as *Z*/*N*, i.e., the electron excess (*Z*) normalized to the NO_2-centers (*N*).[31] As such, the linear trends observed in Figure 8 for both the nitrogen−oxygen and the nitrogen−carbon bonds lead to the conclusion that (a) bond length changes are directly related to the charge on the dinitrobenzenide moiety in general and at the NO_2-centers in particular and (b) the fraction of charge on both NO_2-centers is essentially invariant. Quantitatively, we estimate the relative charges (q_i) on the individual NO_2-centers from their bond lengths with the aid of eq 5 which follows from the classic Pauling bond length/bondorder relationship,[32] i.e.,

$$q_i = 1/n\ \Sigma(d_i - d_0)/(d_1 - d_0) \qquad (5)$$

where d_i is either the N−O or the C−N bond length associated with the relevant NO_2-center, d_0 are those in the neutral acceptor, and d_1 are those in the dinitrobenzenide dianion; the normalization factor *n* accommodates the number of bonds employed in the computation. Based on this analysis of N−O and C−N bond lengths (Table 4), we conclude the fraction of charge *q* on the NO_2-centers in separated ion pairs $K(L_C)^+//DNB^-$ and $K(L_{E1})_2{}^+//DNB^-$ shows the expected symmetrical 0.5/0.5 distribution. On

(31) Thus, $Z/N = 0$, 0.5, and 1.0 for the neutral acceptor, anion radical, and dianion, respectively.

(32) (a) Pauling, L. *Nature of the Chemical Bond*; Cornell: Ithaca, NY, 1960. (b) Le Magueres, P.; Lindeman, S. V.; Kochi, J. K. *J. Chem. Soc., Perkin Trans. 2* **2001**, 1180.

the other hand, the charge distribution in the contact ion pair $K(L_{E3})^+DNB^-$ is calculated to be unsymmetrical, with the charge on the coordinated NO_2-center being about 0.6 and that on the uncoordinated center about 0.4.

(ii) In a similar vein, quinonoidal distortion of the *p*-phenylene bridge[33] can be computed by focusing first on the contraction of its central C−C bond (d_i) upon reduction, so that normalization to the benzene(d_0)/*p*-benzoquinone(d_1) bond length changes provides the measure of the distortion parameter d_q listed in column 3 of Table 4. The corresponding evaluation of quinonoidal distortion based on N−C bond changes[34] is indicated in parentheses. If due cognizance is taken of the semiquantitative nature of such an analysis, we can find no discernible difference in quinonoidal distortion of the dinitrobenzenide moiety despite the unsymmetrical distortion of the charge density between SIP and CIP structures.

(iii) Reduction of the *p*-dinitrobenzene to the anion radical and dianion results in planarization. Thus, the torsion angles β of both NO_2-groups relative to the phenylene bridge in p-dinitrobenzene (Table 1) deviate by approximately 10° from planarity.[35] However, every dinitrobenzenide moiety in Table 4 (entries 1−3) is entirely coplanar with $\beta < 2°$, and the sizable conjugation of NO_2-centers (vide supra) is essentially the same in SIP and CIP ion pairs.

Despite the large (overall) structural changes that accompany SIP and CIP formations, we conclude from such a complete analysis of the X-ray structural data that the electronic interaction between the paired NO_2-centers in dinitrobenzenide is largely unaffected by contact ion pairing. Accordingly, we attribute the observed spectral difference/changes to an electrostatics-induced polarization of the electron-density distribution by the potassium cation, as opposed to the cation-induced electron decoupling between paired NO_2-centers.[36] To determine how such a structural formulation can shed light on the complex spectral changes in the ESR and UV−vis data in Figures 4(5) and 3, respectively, we now return to the earlier development of the two-state (Marcus−Hush) model for dinitrobenzenide anion as a mixed-valence (intervalence) system.[37]

II. Diagnostic Intervalence Transitions in Dinitrobenzenide Ion Pairs as Mixed-Valence Systems. Electronic spectra of separated and contact ion pairs as shown in Figure 3 form the critical link between solid-state structures and solution behavior insofar as they provide topological information about the ground state of the dinitrobenzenide anion as it is subjected to counterion effects. According to Nelsen and co-workers,[13] dinitrobenzenide is a mixed-valence anion in which the paired NO_2/NO_2^- redox centers (with a reorganization energy of $\lambda_v = 1050$ cm^{-1}) are strongly coupled by the sizable electronic coupling element $H_{ab} = 5400$ cm^{-1}. The large magnitude of the ratio $H_{ab}/\lambda = 5.1$ predicts a Robin−Day Class III anion[38] in which the interaction between redox sites is so large that separate NO_2/NO_2^- minima no longer exist, and the unpaired electron is delocalized (barrierless) between both redox centers.[39] Such a ground state is represented by the symmetric potential energy well illustrated in Figure 9, and this single minimum is also largely applicable to the loose dinitrobenzenide in separated ion pairs, owing to minimal influences of the loosely bound counterion.

By way of contrast, the counterion cannot be ignored in contact ion pairs, and cation binding differentiates the paired NO_2-centers sufficient to induce significant polarization.[40] Such an intimately cation-bound dinitrobenzenide remains a Class III anion, with its asymmetric ground-state structure constructed in Figure 9B with λ_v and H_{ab} values that are those applicable to "free" dinitrobenzenide.

Experimental support for the two-state representation of nitrobenzenide ion pairs in Figure 9 (A and B) is best provided by further analysis of the distinctive NIR envelopes (Figure 3) for the separated ion pair versus the contact ion pair. In the former, the most important spectral facet is the vibronic fine structures in free dinitrobenzenide[13] and is reproduced in the separated anion as the characteristic decreasing progression in Figure 3a in both the solution and solid-state spectrum.[41] By way of contrast, in the contact ion pair the vibronic fine structures show a head-and-shoulders progression in which the principal band is not the lowest-energy component but the penultimate one.

According to the two-state model for the free dinitrobenzenide, the principal (0−0) vibronic transition proceeds from the intervalence (delocalized) ground state and is shown in Figure 9A as the most intense (heavy vertical arrow) owing to favorable Franck−Condon factor for the symmetric potential-energy well. The diminished overlap for the secondary (0−1

(33) For previous evaluations of quinonoidal distortion in *p*-phenylene bridged mixed-valence systems, see: Sun, D.-L.; Lindeman, S. V.; Rathore, R.; Kochi, J. K. *J. Chem Soc., Perkin Trans. 2* **2001**, 1585.

(34) (a) The values in parentheses were calculated via eq 5 using two C−N[34b] and six C−C bond lengths of the corresponding dinitrobenzenide. (b) With $d_0 = 1.47$ and $d_1 = 1.36$ Å (single and double C−N bonds, respectively).

(35) A reviewer has suggested that the slight reduction in the torsion angle β that accompanies the reduction of *p*-dinitrobenzene can result from the electrostatic attraction between the negatively charged NO_2-group and ortho-hydrogens.

(36) (a) Due to similarity of the geometries of "free" and ion-paired dinitrobenzenide anions (distances between redox centers, planarities, quinonoidal distortions, etc.), the electronic interactions between the NO_2-centers are expected to be comparable. Their reorganization energies (determined by the same hypothetical noninteracted oxidized and reduced redox centers) are unlikely to differ dramatically.[36b] As such, the H_{ab}/λ_v ratio, which is >10 for "free" dinitrobenzenide,[13] should be significantly larger than unity for ion-paired species. This ensures the absence of a ground-state barrier for electron transfer in ion-paired *p*-dinitrobenzene anion radicals; i.e., they belong to Class III. According to Robin and Day,[38] the basic distinction between mixed-valence complexes lies in their ground-state structure: Class III lying into a single potential well as opposed to the two-well model invoked for Class II. (b) Any variation of the reorganization energies and coupling elements resulting from solvent and counterion effects are moderate (mainly limited to 10−20%, as determined from the intervalence optical transition).[8,36c−e] Thus, such effects can lead to the transformation of Class III into Class II only in the case of borderline systems.[5h,13] (c) Nelsen, S. F.; Tran, H. Q. *J. Phys. Chem. A* **1999**, *103*, 8139. (d) Nelsen, S. F.; Trieber, D. A., II; Ismagilov, R. F.; Teki, Y. *J. Am. Chem. Soc*, **2001**, *123*, 5684. (e) Nelsen, S. F.; Konradsson, A. E.; Clennan, E. L.; Singleton, J. *Org. Lett.* **2004**, *6*, 285.

(37) (a) Marcus, R. A. *Discuss. Faraday Soc.* **1960**, *29*, 21. (b) Marcus, R. A. *J. Phys. Chem.* **1963**, *67*, 853. (c) Marcus, R. A.; Sutin, N. *Biochim. Biophys. Acta* **1985**, *811*, 265. (d) Hush, N. S. *Trans. Faraday Soc.* **1961**, *57*, 557. (e) Hush, N. S. *Prog. Inorg. Chem.* **1967**, *8*, 391. (f) Hush, N. S. *Electrochim. Acta* **1968**, *13*, 1005. (g) Sutin, N. *Prog. Inorg. Chem.* **1983**, *30*, 441. (h) Brunschwig, B. S.; Sutin, N. *Coord. Chem. Rev.* **1999**, *187*, 233.

(38) Robin, M. B.; Day, P. *Adv. Inorg. Chem. Radiochem.* **1967**, *10*, 247.

(39) (a) Compare similar barrierless electron transfer in strongly coupled donor/acceptor dyads in arene charge-transfer complexes with nitrosonium.[39b,c] (b) Rosokha, S. V.; Kochi, J. K. *J. Am. Chem. Soc.* **2001**, *123*, 8985. (c) Rosokha, S. V.; Kochi, J. K. *New J. Chem.* **2002**, *26*, 851.

(40) For an earlier example of counterion induced polarization, see: Sun, D.-L.; Rosokha, S. V.; Lindeman, S. V.; Kochi, J. K. *J. Am. Chem. Soc.* **2003**, *125*, 15950.

(41) See: (a) Risko, C.; Barlow, S.; Coropceanu, V.; Halik, M.; Brédas, J.-L.; Marder, S. R. *Chem. Commun.* **2003**, 194. (b) Bailey, S. E.; Zink, J. I.; Nelsen, S. F. *J. Am. Chem. Soc.* **2003**, *125*, 5939 for examples of vibronic-splitting analysis in mixed-valence systems.

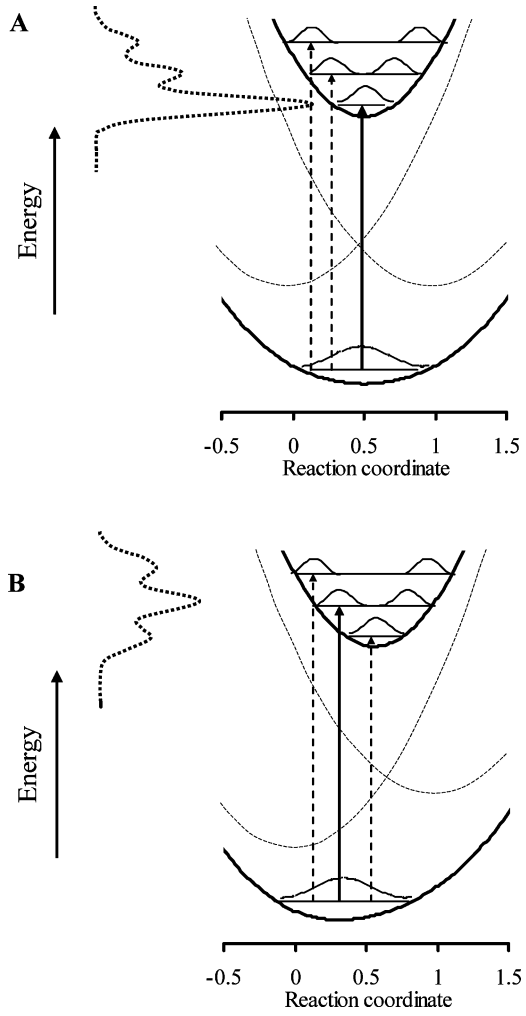

Figure 9. Two-state representations of a (A) "separated" ion pair and (B) "contact" ion pair of dinitrobenzenide showing the principal intervalence transitions (heavy vertical arrows) from symmetric and asymmetric ground states, respectively. The constructed NIR envelopes are illustrated by dashed curves on the left sides of the drawings to be compared with the experimental spectra in Figure 3a and c, respectively.

and 0−2) transitions predict the decreasing progression of resolved vibronic bands found in the experimental spectrum, as illustrated by the constructed NIR spectrum on the left side of the drawing to be compared with the experimental spectrum in Figure 3a.

The two-state model also accommodates the contact ion pair via the distortion of the intervalence ground state by electrostatic polarization (vide supra). The resulting asymmetric potential-energy well is qualitatively drawn (Figure 9B) to depict the skewed spin distribution between the paired NO_2/NO_2^- redox centers.[42] Such a desymmetrization is tantamount to a shift of the intervalence ground state (Figure 9B) so that the (0−1) transition is the most probable, as depicted by the heavy vertical arrow, and the associated (0−0 and 0−2) transitions are consequently the minor ones. The constructed NIR envelope of the "contact" dinitrobenzenide is illustrated on the left side of the drawing to reflect its striking similarity to the experimental spectrum in Figure 3c.[43] Finally, the intermediate NIR spectrum of the contact ion pair for the dicyclohexano-18-crown-6 complex (Figure 3b) is a result of the partial charge redistribution measured in the X-ray structure (Table 1, entry 3). By interpolation, the constructed spectrum of $K(L_{E3})^+DNB^-$ results from the two-state model when the minor shift in the somewhat asymmetric (0.6/0.4) ground state merely attenuates the (0−0) transition, consistent with the experimental observation of the reduced 910-nm intensity in Figure 3b.

The meaningful comparison of separated and contact ion pairs provided by the success of the two-state model for the optical changes ensures the direct applicability of the quantitative X-ray structures to these highly labile species in solution. As such, we can now turn to the ESR studies in Figures 5 and 6 with the assurance that they faithfully reflect the structural changes between separated and contact ion pairs in solution, especially as their equilibria are finely modulated by rather small variations in temperature.

III. Dynamic Equilibria of "Contact" Ion Pairs. The selective (alternating) line broadening behavior in the ESR spectrum of contact ion pairs derived from the dicyclohexano-18-crown-6 and 18-crown-6 complexes $K(L_{E3})^+$ and $K(L_{E2})^+$, respectively, in THF solution (Figure 6) reflects the fast redistribution of partial spin densities between the two NO_2/NO_2^- centers. Phenomenologically, such a dynamic effect is similar to a rapid intramolecular electron transfer, and the temperature-dependent line broadening allows the self-exchange process to be evaluated (vide supra). However, dinitrobenzenide is a Robin−Day Class III anion, and the large electronic coupling H_{ab} relative to the reorganization energy λ_v is sufficient to nullify any such (intra-anion) activation barrier,[44] and the spin redistribution must perforce be attributed to some other time-dependent phenomenon. In view of the tight cation binding in this system, we attribute the dynamic line broadening to the migration of the potassium counterion from one "contact" nitro-center to the other (uncoordinated) site, simultaneous with spin redistribution. The interchange can be pictorially depicted as

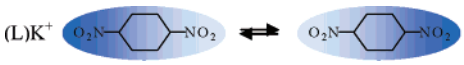

(6)

and it is strongly reminiscent of an intramolecular self-exchange rate process in a simple Class II anion, not mediated by the counterion.[45]

The mechanism of the cation-interchange process in eq 6 can occur via the continuous migration of the complexed K^+ across the surface of the anion by always maintaining its "contact" characteristics intact. However, the ESR observation of the

(42) Interaction of potassium with one of the NO_2-centers in ion-paired mixed-valence anions results in the stabilization (vertical shift) of one of the (parabolic) diabatic states and leads to the corresponding transformations of the adiabatic ground and excited states in Figure 9B (constructed with the two-state model[37] using the same H_{ab} and λ values as those in the symmetric system in Figure 9A).

(43) (a) The quantitative analysis of this vibronic splitting awaits time-dependent quantum mechanical calculations such as those described earlier.[13,41] See: (b) Zink, J. I.; Shin, K.-S. *Advanced Photochemistry*; Wiley: New York, 1991; Vol. 16, p 119. (c) Schatz, P. N. In *Inorganic Electronic Structure and Spectroscopy*; Solomon, E. I., Lever, A. B. P., Eds.; Wiley: New York, 1999; Vol. II, p 175. (d) Piepho, S. B.; Krausz, E. R.; Schatz, P. M. *J. Am. Chem. Soc.* **1978**, *100*, 2996. (e) Simoni, E.; Reber, C.; Talaga, D.; Zink, J. I. *J. Phys. Chem.* **1993**, *97*, 12678. (f) Coropceanu, V.; Malagoli, M.; Andre, J. M.; Brédas, J. L. *J. Chem. Phys.* **2001**, *115*, 10409.

(44) (a) In the absence of the intrinsic barrier related to the Marcus reorganization energy, the usual expression of the electron-transfer rate constant[44b] is not applicable. (b) $k_{et} = k\nu_n \exp(-\Delta G^*/RT)$, where k is the electronic transmission coefficient, ν_n is the nuclear vibration frequency, and $\Delta G^* = (\lambda - 2H)^2/4\lambda$ is the free energy of activation.[37]

(45) Due to such a similarity, the (solvent-dependent) ESR line-broadening of *p*-dinitrobenzene anion radical was earlier interpreted as Class II electron transfer. See: Telo, J. P.; Grampp, G.; Shohoji, M. C. B. L. *Phys. Chem. Chem. Phys.* **1999**, *1*, 99.

separated ion pair at very low temperatures shows that this loose species is thermodynamically viable, most likely as a result of the enhanced solvation of the complexed cations $K(L_{E3})^+$ and $K(L_{E2})^+$ by THF solvent at low temperature.[46] The latter favors the dynamic spin redistribution to more likely be a two-state process that proceeds via the separated ion pair, i.e.,

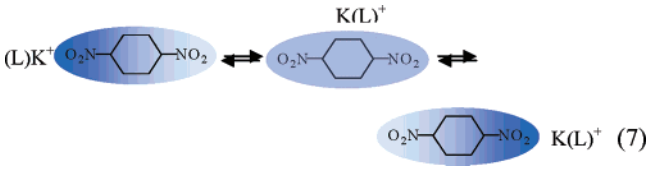

(7)

The relatively fast kinetics of the spin redistribution of $k_{ex} \approx 10^9\ s^{-1}$ and moderate thermodynamic parameters of $\Delta H^{\neq}_{ex} = 0.8$ kcal mol^{-1} and $\Delta S^{\neq}_{ex} = -5$ eu suggest that the rate of ion-pair dissociation is rate-limiting.

In ion pairs mediated by alkali-metal cations, such an ion separation will be dependent on the polyether complexon, which in our system is expected to be[47]

$$K(L_{E1})^+ > K(L_{E2})^+ \approx K(L_{E3})^+ > K(L_{E4})^+$$

In qualitative accord with these expectations, the temperature-dependent ESR spectrum of the dibenzo-18-crown-6 complex as the contact ion pair salt $K(L_{E4})^+DNB^{-\bullet}$ dissolved into THF (Figure 5) reveals the presence of two isomeric contact ion pairs identified as CIP_1 and CIP_2 (eq 1) in equilibrium with the separated ion pair (SIP). The absence of the temperature-dependent line broadening in the ESR spectrum of CIP_1 indicates that ion-pair dissociation is slow relative to spin redistribution, but the difference is less in CIP_2 which clearly shows a limited line broadening behavior (without alternation). We attribute this difference to the existence of two types of ion-pairing binding of the $K(L_{E4})^+$ cation to DNB^- anion in solution, with one type showing tighter binding than the other. If so, tighter ion-pair binding can be speculatively presented as the symmetrical (bidentate) structure,[23]

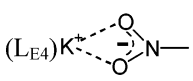

CIP_1

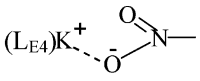

CIP_2

and the looser ion-pair binding is depicted on the right. Experimentally, these types of symmetric and unsymmetric ion-pair bindings are indeed inherent to the X-ray structures of the "contact" dianion and anion, as illustrated in Figure 2B and A, respectively. Furthermore, the activation barrier between CIP_1 and CIP_2 is sufficient to preclude a general ESR line broadening, although their exchange is likely to proceed via a preequilibrium dissociation observed in the low-temperature (193 K) spectrum in Figure 5, i.e.[48]

$$CIP_1 \overset{K_{SEP}}{\rightleftharpoons} SIP \overset{K^{-1}_{SEP}{}'}{\rightleftharpoons} CIP_2 \qquad (8)$$

If so, the rate of isomerization between CIP_1 and CIP_2 in eq 1 is controlled by their thermodynamics stabilization.

Summary and Conclusions

The distinctive structures of "separated" and "contact" ion pairs are unambiguously identified in Figures 1 and 2, respectively, through X-ray crystallography of dinitrobenzenide (DNB^-) salts of potassium complexed with either a three-dimensional [2,2,2]-cryptand ligand (L_c) or various two-dimensional crown-ethers (L_E) in Chart 1. These ion-pair structures are also spectrally characterized by their own unique NIR bands (Figure 3a−c) with resolved vibronic splittings arising from intervalence transitions in dinitrobenzenide as a strongly coupled mixed-valence anion. Most importantly, the same diagnostic vibrational fine structures of each ion-pair salt dissolved into THF ensure that these "separated" and "contact" ion-pair structures also persist in solution.

Comparative spectral analysis shows that dinitrobenzenide as "separated" ion pairs in THF solution is equivalent to the "free" anion in polar DMF, previously assigned with the aid of the Marcus−Hush two-state model to a strongly coupled Robin−Day Class III intervalence system. It is thus noteworthy that the experimental X-ray structure in Table 1 as well as the ESR spectrum in Figure 4a confirms the single potential-energy ground state for "separated" dinitrobenzenide, with its odd electron lying in a *symmetric* minimum equally distributed between both NO_2-centers. Contrastingly, X-ray and ESR structure analyses of the "contact" ion pair establish an *asymmetric* ground state for dinitrobenzenide with the charge electrostatically skewed (polarized) toward that NO_2-center directly paired to the potassium counterion. Otherwise, the two-state analysis of the spectral NIR band in Figure 9B predicts the electronic coupling between the paired NO_2-centers to be essentially the same as that in "free" dinitrobenzenide or as the "separated" ion pair.

Such intact characteristics of dinitrobenzenide anion upon contact ion pairing with different complexed potassium counterions $K(L_E)^+$ can be directly observed as at least four types of dynamic effects in their temperature-dependent ESR spectra. Thus, among the various crown-ether ligands, the dibenzo-18-crown-6 complex as $K(L_{E4})^+$ is the least prone to separate from dinitrobenzenide anion, and two isomeric contact ion pairs (CIP_1 and CIP_2) undergo facile interchange via the separated ion pair (SIP) in eq 2. On the other hand, K^+ complexed to either 18-crown-6 as $K(L_{E2})^+$ or dicyclohexano-18-crown-6 as $K(L_{E3})^+$ is substantially more prone to separate from dinitrobenzenide anion. The fast dynamic process for CIP_3 is observed in the temperature-dependent ESR spectra (Figure 6) as a selective line broadening leading to the site exchange in eq 3, and the pathway for electron redistribution is again preferentially viewed as ion-pair separation in eq 4. As expected for such differences

(46) (a) The low-temperature dissociation of ion-paired anion radicals can result from favorable counterion solvation; see ref 28b. (b) In eqs 2 and 4, SIP formation may result in the further deligation of $K(\mathbf{L}_E)^+$ by THF as an ethereal (donor) solvent. This is indicated by the value of formation constant of $K(\mathbf{L}_{E4})^+$: log K ≈ 2 in 50% aqueous THF.[46c] (c) Rechnitz, G. A.; Eyal, E. *Anal. Chem.* **1972**, *44*, 370.

(47) (a) Such an order agrees (i) with dissociation equilibria that show enhanced shifts to "free" anion radicals in solution with $K(L_{E3})^+$ or $K(L_{E2})^+$ as compared to those with $K(L_{E4})^+$ and (ii) with the vibronic-splitting analysis of the NIR intervalence absorption. Therefore, the rate of the intramolecular exchange processes that are directly related to the strength of $DNB^-/K(L)^+$ interaction) is much slower in ion pairs with the $K(L_{E4})^+$ counterion. This results in the weak line-broadening of the ESR spectrum of CIP_2 as compared to those in systems with either $K(L_{E3})^+$ or $K(L_{E2})^+$ counterions. (b) Similarly, picrate anion was found earlier to be bound more strongly to $K(L_{E4})^+$ than to $K(L_{E2})^+$. See: Yatsimirskii, K. B.; Talanova, G. G. *Dokl. Chem.* **1983**, *273*, 414.

(48) Alternatively, the dissociation of one of the ionic K−O bonds may lead to the direct transformation of CIP_1 into CIP_2, followed by further dissociation into SIP.

Table 5. Crystallographic Parameters of the Ion-Pair Salts[a]

parameter	$K(L_C)^+DNB^-$	$K(L_{E1})_2^+DNB^-$	$K(L_{E3})^+DNB^{-b}$	$[K(L_{E2})^+]_2DNB^{2-}$
a, Å	18.2320(9)	12.1156(6)	16.027(4)	20.411(3)
b, Å	11.6937(6)	12.8981(7)	14.913(4)	8.321(1)
c, Å	13.9494(7)	12.9427(7)	23.619(8)	22.718(4)
α, deg	90	111.682(1)	90	90
β, deg	107.036(1)	91.833(1)	90	103.938(4)
γ, deg	90	110.057(1)	90	90
V, Å^3	2844	1736	5645	3745
F(000)	1244	786	2472	1648
μ, mm^{-1}	0.25	0.23	0.25	0.32
ρ, g/cm^3	1.363	1.423	1.364	1.375
reflections	9653	10834	75582	8958
independent	9251	10834	5547	8459
observed ($F > 4\sigma$)	8015	8786	2194	5576
parameters	512	636	352	659
R ($F > 4\sigma$)	0.0386	0.0471	0.0497	0.0542
wR_2	0.1054	0.1240	0.1107	0.1513
GOF	1.053	1.045	0.740	1.030

[a] Data collected at 123 K, unless noted otherwise. [b] At 173 K.

between $K(L_{E4})^+$ and either $K(L_{E2})^+$ or $K(L_{E3})^+$, the ultimate ion-pair separation to SIP favors CIP_3 over CIP_1 or CIP_2, as established by the series of comparative (temperature-dependent) ESR spectra in Figures 5 and 6 as well as the UV−vis spectral changes in Figures 7 and S8.

In a more general context, the apparent spin "localization" observed in the ESR spectra of dinitrobenzenide indicates that strongly coupled Class III systems upon contact ion pairing can exhibit spectral features that are commonly ascribed to localized intervalence Class II systems. As such, it is important to emphasize the caveat that dynamic ion-pairing effects must always be quantitatively taken into account in the assignment/interpretation of experimental data, especially of charged (ionic) mixed-valence systems at the Class III/II border that have recently received increased attention.[4h,9]

Experimental Section

Materials. Metallic potassium from Aldrich was stored in a drybox and used without additional purification. The crown-ethers benzo-15-crown-5, 18-crown-6, dicyclohexano-18-crown-6, dibenzo-18-crown-6, and [2,2,2]cryptand (4,7,13,16,21,24-hexaoxa-1,10-diazabicyclo-[8.8.8]hexacosane) from Aldrich were also used as received. *p*-Dinitrobenzene (DNB) from Aldrich was sublimed twice and recrystallized from ethanol and dried in vacuo. High purity tetrahydrofuran from Merck was freshly distilled from sodium/benzophenone under an argon atmosphere and briefly stored over potassium or sodium mirror. Hexane from Merck was successively washed with concentrated HNO_3/H_2SO_4, H_2O, NaOH, and H_2O, dried over $CaCl_2$ followed by distillation from sodium/benzophenone, and stored under argon atmosphere. Ethylene glycol dimethyl ether (DME) from Sigma-Aldrich was freshly distilled from sodium/benzophenone and stored under an argon atmosphere. *p*-Dinitrobenzene-d_4 was synthesized from nitrobenzene-d_5 (Aldrich, 99.5 atom % D) by standard reduction, acetylation, and nitration procedures to afford *p*-nitroaniline-d_4 followed by Cu catalyzed reoxidation to *p*-dinitrobenzene-d_4 in the presence of $NaNO_2$ and HBF_4.[49] Isolated yield: 40%; pale yellow crystals; *m*/*z*, 172; mp, 173−5 °C.

Preparation of Ion-Pair Salts of *p*-Dinitrobenzene Radical Anions: *p*-Dinitrobenzene was reduced with potassium mirror in the presence of cryptand or crown ethers as follows. Potassium metal (7 mg, 0.179 mmol) was carefully cleaned mechanically in a glovebox under an argon atmosphere and placed in a well-dried Schlenk tube (50 mL). The tube was slowly heated with an oil bath in a vacuum (10^{-3} Torr) until complete sublimation of the metal and mirror formation on the wall were apparent. In another Schlenk tube, a sample of *p*-dinitrobenzene (30 mg, 0.178 mmol) together with a stoichiometric amount (0.178 mmol) of the complexon (either cryptand or crown ethers) was degassed by melting in high vacuo (10^{-3} Torr). The degassed mixture was dissolved in 20−25 mL of dry THF, and the solution was transferred into the Schlenk tube containing the metal mirror. An intense green coloration appeared immediately. The solution was allowed to stand at −20 °C for a few days until the reduction was complete (potassium mirror disappeared completely). The resulting greenish solution was carefully covered with a layer of dry hexane (20 mL) and placed for 2−3 days in a constant-temperature cooler maintained at −60 °C. The reaction batch typically yielded 5−10 mg of well-formed crystals growing on the walls at the interface where the solvents diffuse together. The highly air-sensitive, dark green/or brown crystals (Table S1) were carefully collected and then used for the X-ray structural analysis and IR studies (see IR spectra in Figure S9 in Supporting Information) as well as (after dissolving in dry THF) for ESR and UV−vis spectroscopic measurements.

Preparation of *p*-Dinitrobenzene Dianion Salt. The dinitrobenzenide dianion was prepared by the procedure employed for the anion radical except 2−3 molar equivalents of crown ether and potassium relative to DNB were used.

X-ray Crystallography of Ion-Pair Salts. The single crystals of the ion-pair salts were obtained at −60 °C by the slow diffusion of hexane carefully layered on the top of the corresponding saturated THF solutions. The diffraction data for all the ion-pair salts were collected with the aid of a Siemens/Bruker SMART diffractometer equipped with an APEX CCD detector using Mo Kα radiation (λ = 0.710 73 Å), either at −150 or −100 °C. In all cases, semiempirical absorption correction was applied.[50] The structures were solved by direct methods[51] and refined by a full matrix least-squares procedure[52] with IBM Pentium and SGI O_2 computers (see Table 5). [The X-ray structure details of various compounds are on deposit and can be obtained from the Cambridge Crystallographic Data Center, U.K.]

ESR Measurements. The electron spin resonance measurements were performed on a Bruker ESP-300 X-band spectrometer with 100 kHz field modulation, 0.1 to 0.2 G modulation amplitude, and 20 mW microwave power. The THF solutions were prepared in a Schlenk tube

(49) Blatt, A. H, Ed. *Organic Synthesis*; Wiley: New York, 1961; Vol. 2, p 225.
(50) Sheldrick, G. M. *SADABS*, version 2.03; Bruker/Siemens Area Detector Absorption and Other Corrections. Bruker X-ray Analytical Systems: Madison, Wisconsin, 2000.
(51) Sheldrick, G. M. *SHELXS 97*, Program for Crystal Structure Solutions; University of Göttingen: Germany, 1997.
(52) Sheldrick, G. M. *SHELXL 97*, Program for Crystal Structure Refinement; University of Göttingen: Germany, 1997.

kept at −40 °C then transferred into a quartz ESR tube (2-mm diameter) under an argon atmosphere. The tube was placed in a quartz Dewar set in the center of a rectangular cavity, with the temperature regulated by an IBM control unit to ±0.5 °C. Dry compressed nitrogen was pumped through the cavity to avoid condensation of adventitious moisture at the low (below 0 °C) temperature. The calculation of hyperfine splitting constants was carried out by the computer simulation of the ESR spectra with a Bruker WINEPR Simfonia program (version 1.25). Alternatively, the THF solution of crystals obtained from a series of crown ethers also showed well-resolved ESR spectra, as those crystals that are not stable at room temperature and also their solutions were kept at −40 °C under an argon atmosphere for ESR measurements. On the other hand, *p*-dinitrobenzene radical anion salts with different crown ethers were also prepared in situ by exposing the DNB solution to a potassium mirror attached to the wall of the ESR tube. Both crystal and in situ prepared solutions of a patrticular radical anion were measured by ESR, the results were in good agreement, and the hyperfine splitting constants obtained from the spectra are listed in Table 3.

Measurement of Electronic Spectra. All spectroscopic measurements were performed under an argon atmosphere in a 1-mm or 1 cm quartz cuvette on either a Hewlett-Packard 8453 diode-array or a Varian Cary 5 spectrometer. In each case, freshly prepared THF solutions of the corresponding ion-pairs salts were made up in a rigorously air-free drybox, or in a Schlenk tube under argon at −40 °C. The samples for in situ measurements were prepared by exposing the solution to potassium mirror inside the UV cuvette at a temperature of −20 °C. The reaction was spectroscopically monitored for completion by following the changes in concentration of the neutral *p*-dinitrobenzene which has an absorption peak at 266 nm. For solid-state measurements, 2 or 3 mg of crystals of the corresponding ion-pair salts were added to a drop of mineral oil (ca. 0.1 mL) attached to a glass slide, and the crystals were ground between two glass plates to a fine powder and the absorption measurements were taken.

IR Measurements. Crystalline samples of the ion-pair salts were mounted directly on the germanium sampling plate of the single-reflection HATR (Smart Miracle, Pike Technology) under an argon atmosphere, and the infrared spectra (Figure S9) were measured with a Nexus 470 FT-IR (Thermo Nicolet). Alternatively, crystals for X-ray crystallographic analysis suspended in mineral oil were used (and the mineral oil background subtracted digitally).

Acknowledgment. We thank Professor S. F. Nelsen for kindly providing us with a copy of the ESR-EXN program, M.G. Davlieva for isolation of the crystalline salts of $K(L_C)^+//DNB^-$ and $[K(L_{E2})^+]_2DNB^{2-}$, S. M. Dibrov for crystallographic assistance, and the R. A. Welch Foundation for financial support.

Supporting Information Available: X-ray crystallographic files in CIF format. Crystallization details and physical properties of ion pair salts (Table S1); thermodynamics of the CIP_1/CIP_2 isomerization of $K(L_{E4})^+DNB^-$ (Figure S1); temperature-dependent ESR spectrum of $K(L_{E3})^+DNB^-$ (Figure S2); dynamic ESR simulation of alternating line-broadening for $K(L_{E3})^+DNB^-$ (Figure S3); simulation of low-temperature ESR spectrum of $K(L_{E3})^+DNB^-$ as superposition of CIP and SIP ion pairs (Figure S4); simulation of low-temperature ESR spectrum of $K(L_{E4})^+DNB^-$ as superposition of CIP and SIP ion pairs (Figure S5); temperature-dependent ESR spectrum of $K(L_{E2})^+DNB^-$ (Figure S6); temperature-dependent ESR spectrum of $K(L_{E2})^+DNB\text{-}d_4^-$ (Figure S7); temperature-dependent electronic spectrum of $K(L_{E2})^+DNB^-$ (Figure S8); and IR spectra of crystalline ion pair salts (Figure S9). This material is available free of charge via the Internet at http://pubs.acs.org.

JA043998X